한국기계가공학회지, 제20권, 제9호, pp. 11～19(2021.09) ISSN 1598-6721(Print)
Journal of the Korean Society of Manufacturing Process Engineers, Vol. 20, No. 9, pp. 11~19(2021.09) ISSN 2288-0771(Online)

https://doi.org/10.14775/ksmpe.2021.20.09.011

Finite Element Analysis of the Effects of Process and Material Parameters on the LVDT Output Characteristics

Young-Soo Yang*, Kang-Yul Bae**,#
*Department of Mechanical Engineering, JNU, **Department of Mechatronics Engineering, GNU

LVDT의 출력 특성에 미치는 공정 및 재료 변수의 영향에 관한 유한요소해석

양영수*, 배강열**,#
*전남대학교 기계공학과
**경상국립대학교 메카트로닉스공학과

(Received 25 June 2021; received in revised form 20 July 2021; accepted 22 July 2021)

ABSTRACT

Linear variable differential transformer (LVDT) is a displacement sensor and is commonly used owing to its wide measurement range, excellent linearity, high sensitivity, and precision. To improve the output characteristics of LVDT, a few studies have been conducted to analyze the output using a theoretical method or a finite element method. However, the material properties of the core and the electromagnetic force acting on the core were not considered in the previous studies. In this study, a finite element analysis model was proposed considering the characteristics of the LVDT composed of coils, core, magnetic shell and electric circuit, and the core displacement. Using the proposed model, changes in sensitivity and linear region of LVDT according to changes in process and material parameters were analyzed. The outputs of the LVDT model were compared with those of the theoretical analysis, and then, the proposed analysis model was validated. When the electrical conductivity of the core was high and the relative magnetic permeability was low, the decrease in sensitivity was large. Additionally, an increase in the frequency of the power led to further decrease in sensitivity. The electromagnetic force applied on the core increased as the voltage increased, the frequency decreased, and the core displacement increased.

Key Words : LVDT(선형가변차동변압기), Output Characteristic(출력 특성), Supply Power(공급 전원), Core Material(코어 재질), Finite Element Analysis(유한요소해석)

1. Introduction

A linear variable differential transformer (LVDT) is a displacement measurement sensor comprising coils and a core and has widespread and diverse applications owing to its wide measurement range, excellent linearity, and high sensitivity and precision[1-4]. LVDTs can be produced in various forms because of their simple structure and the lack

Corresponding Author : kybae9@gnu.ac.kr
Tel: +82-55-772-3384, Fax: +82-55-772-3389

of standardized specifications[5], and some studies have used theoretical methods to analyze the output voltage according to the displacement of the core. In these studies, the design parameters were adjusted by manipulating the relationships between the parameters and the output to expand the sensitivity and linear region; the magnetic conductance was defined while considering the geometric shape in order to apply the method of calculating the mutual inductance; or a method was used wherein the voltage induced in the secondary coils was derived by inducing a magnetic flux density generated from the core and evaluating the time change of the magnetic flux[4,6-8]. These analyses cannot be applied when the displacement of the core increases and deviates from the secondary coils. Furthermore, if the end of the core is close to the edge of the secondary coil, the accuracy level of the analysis becomes low[3]. In contrast, a finite element method can be used to analyze the magnetic flux and voltage between the coils according to the design parameters of the LVDT. The finite element analysis can be used to easily identify the effects of environmental conditions, which is difficult to realize theoretically or experimentally, and the results thus obtained are highly consistent with the output characteristics of the fabricated product[2-4]. Nevertheless, existing studies have not taken into consideration the characteristics of the material, such as the core's electrical conductivity, and did not comprise an analysis of the effect of the power supply, although the generation of electromagnetic force was expected.

Ferrite is mainly used for the fabrication of cores, but owing to its significant drawbacks, such as high brittleness and low strength when a change in the geometric form is required, studies have been conducted to investigate alternative materials[9]. If a different core material is used, it is necessary to investigate the effects of an eddy current by its electrical conductivity[10]. Furthermore, if the core is moved, an electromagnetic force is generated, which may adversely affect the measurement of LVDT[10]. This study presents a finite element analysis model that takes into consideration the output characteristics of an LVDT, and the model is validated by supplementing the theoretical solutions suggested in existing studies. Using the proposed model, we analyzed the changes in the sensitivity and the linear region according to changes in the process and material parameters and analyzed the electromagnetic force of the core according to the process parameters.

2. LVDT Modeling and Analysis

2.1 Theoretical Model

As shown in Fig. 1(a), an LVDT consists of a primary coil, two secondary coils (secondary coils 1 and 2, respectively) on the left and right sides, a core that moves along the axis from the core center, and a magnetic shell that wraps over the coils. In terms of the geometric parameters, the core

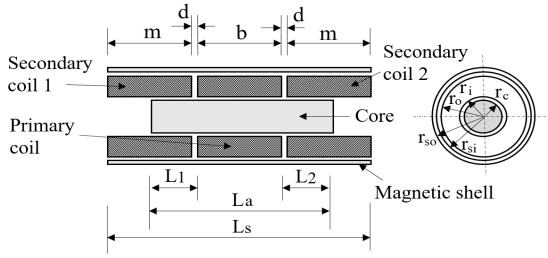

(a) Sectional drawing

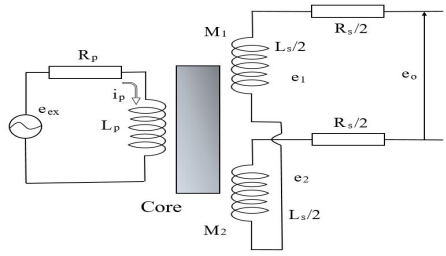

(b) Equivalent electrical circuit

Fig. 1 Schematic model of LVDT

radius is denoted by r_c, length by L_a, outer radius of the coil by r_o, inner radius by r_i, primary coil width by b, secondary coil width by m, gap between the coils by d, length of the magnetic shell by L_s, and inner and outer radii by r_{si} and r_{so}, respectively.

The LVDT can be simplified into an electrical model consisting of a power source, resistance, and coils, as shown in Fig. 1(b). Here, e_{ex} represents a power supply that has a frequency f with a root mean square (rms) of E, R_p is the resistance of the primary coil, L_p is the self-inductance of the primary coil and core system (primary coil system), i_p is the current of the primary coil, M_1 is the mutual inductance of the primary coil and secondary coil 1, and M_2 is the mutual inductance of the primary coil and secondary coil 2. L_s is the overall inductance of the secondary coils, R_s is the overall resistance of the secondary coils, and e_o is the output voltage.

In Fig. 1(b), while assuming that the value of R_p is negligible as compared to the load resistance of the output side, the output voltage can be expressed as follows[5]:

$$e_o = E\frac{M_1 - M_2}{L_p} \tag{1}$$

If the mutual inductance of the primary coil and each secondary coil and the self-inductance of the primary coil system are induced, the output voltage can be calculated using Eq. (1). The mutual inductance can be obtained by determining the distribution of the magnetic flux leakage on the core surface across L_1 and L_2 and the total magnetic flux that passes through the secondary coil[7,8]. The self-inductance of the primary coil system can be determined using the relationship between the magnetic flux and inductance. In this method, the voltage induced in secondary coil 1 is obtained as follows.

$$\begin{aligned} e_1 &= E\frac{M_1}{L_p} + e_i = 2\pi f I_p M_1 + e_i \\ &= \frac{\pi^2 f \mu_0 I_p N_p N_s}{\ln(\frac{r_o}{r_i})} \bullet \frac{(2L_2 + b)x_1^2}{mL_a} + e_i \end{aligned} \tag{2}$$

where, N_p and N_s are the number of windings of the primary and secondary coils, respectively; μ_o is the permeability of air; and x_1 is the superimposed length of the core and secondary coil 1. e_i is the basic induced voltage, which can be calculated based on the value of $e_i = EM_o/L_p$, and M_o is the mutual inductance of the primary coil with a core and the air-cored secondary coil without a core. The voltage induced in secondary coil 2 can also be calculated using the aforementioned method.

2.2 Finite Element Model and Analysis

A finite element analysis model for simulating the characteristics of an LVDT is proposed with the use of the software FLUX[11] and is used to analyze the output voltage characteristics according to the process and material parameters.

Fig. 3(a) presents the finite element division of the core and magnetic shell region. Based on the symmetry of the analyzed object, we set the analyzed region as one-fourth of the model. Fig. 3(b) presents a finite element model that comprises non-meshed coils. Around the LVDT, we set an infinite cylinder having a diameter of 120 mm and length of 240 mm, which was the range determined to be unaffected by the magnetic flux and set the internal empty space as an air region. In the analysis region, we divided the core and the magnetic shell into 0.7-mm elements in the length direction from the edge, 0.4-mm elements in thecircumferential direction, and 0.25-mm elements

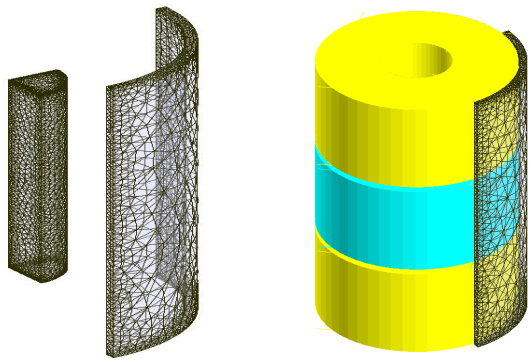

(a) Core and magnetic shell (b) With coils

Fig. 2 Solution domain of finite element model for LVDT analysis

in the radial direction from the edge; the infinite cylinder was divided into 10-mm elements in the length direction from the edge and 10-mm elements in the circumferential direction, which resulted in approximately 70,000 tetrahedral elements. Table 1 lists the default values and variable values of the process and the material parameters applied to the analysis of the LVDT characteristics. The analysis was performed by setting the design parameters consistently as shown in Table 2.

To simulate the characteristics based on the core displacement, we analyzed the voltage value of each secondary coil while moving the core position from −40mm to 40 mm at 1-mm intervals when the position of the center is 0.

Table 1 Process and material parameters for LVDT analysis

Parameter	Value	Variation
Supply voltage(rms), V	5	4 ~ 12
Supply frequency, Hz	2,000	60 ~ 5,000
Relative permeability of core	5,000	1,000 ~ 20,000
Conductivity of core, S/m	8.33	8.33 ~ 6.67E6
Relative permeability of shell	5,000	5,000
Conductivity of shell, S/m	8.33	8.33

Table 2 Design parameters for LVDT analysis

Parameter	Value
Coil width, mm	32
Inner radius of coil, mm	10.5
Outer radius of coil, mm	29.5
No. of coil turns	1,000
Radius of core, mm	10
Length of core, mm	70
Distance between coils, mm	2
Inner radius of shell, mm	30
Thickness of shell, mm	2
Length of shell, mm	100

3. Results and Discussion

Fig. 3 presents the results of the theoretical analysis and the finite element analysis for the case wherein the power supply has a voltage of 5 V and frequency of 2,000 Hz, and the core's relative permeability is 5,000 with non-conductivity. It shows the voltage and the differential voltage at secondary coils 1 and 2 at the same time according to the displacement of the core. The theoretical analysis was performed for up to a displacement of ±19 mm, which was the maximum displacement that could be analyzed, and the finite element analysis

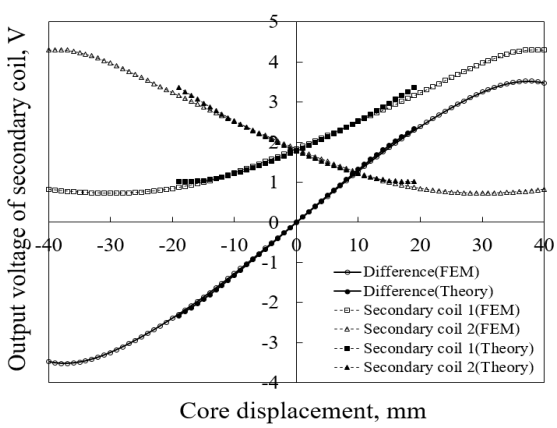

Fig. 3 Output voltages with changes of core displacement

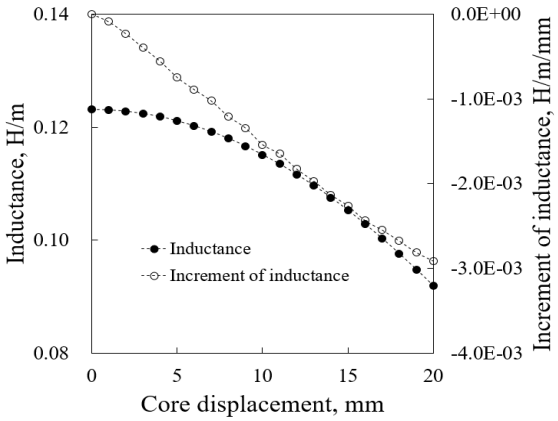

Fig. 4 Self-inductance of primary coil and core system and its increment with changes of core displacement

was performed for up to ±40 mm. In the region wherein the displacement is small, the differential voltages appear linear, and the results of the finite element analysis and theoretical analysis are very similar.

Fig. 4 presents the self-inductance of the primary coil system. It decreases as the displacement of the core increases, and its slope increase linearly in the negative direction. As shown in Eq. (2), the voltage induced in a secondary coil is caused by the increase in the mutual inductance and the decrease in the self-inductance, both of which are proportional to the square of the core displacement. The output characteristics of the LVDT can be expressed using the relationship between the core displacement and output voltage. For this, we define the sensitivity and linear region. In the linear region (±5 mm), we defined the output per unit distance as sensitivity.

$$Sensitivity,\ V/mm = \frac{Change\ of\ output\ voltage,\ V}{Change\ of\ core\ position,\ mm} \quad (3)$$

The linear region is defined as twice the core displacement, wherein the error rate between the output voltage and the linear slope line (percentage

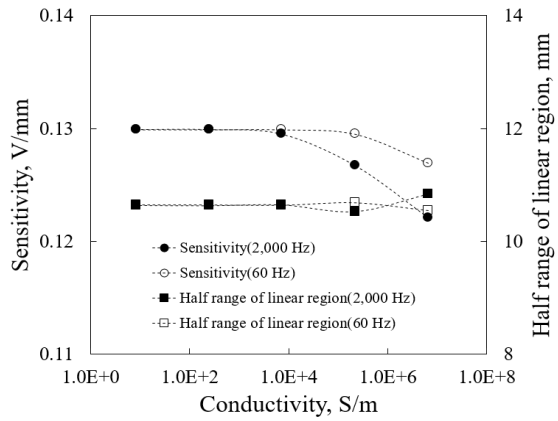

(a) Conductivity

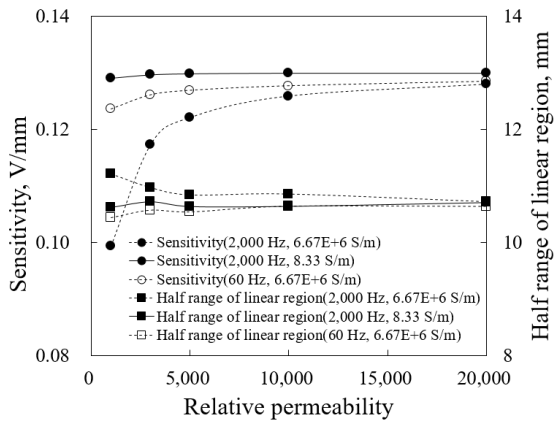

(b) Permeability

Fig. 5 Sensitivity and linear region with changes of material parameter

of the different between the output and linear value in the total output) is less than or equal to 1%.

$$Error\ rate,\ \% = \frac{|Output\ voltage - Core\ displacement \bullet Sensitivity|}{Maximum\ core\ displacement \bullet Sensitivity} \times 100$$

$$Linear\ region,\ mm = 2 \times core\ displacement\ of\ 1\%\ error\ rate \quad (4)$$

Here, the maximum core displacement = L_1.

Fig. 5(a) presents the sensitivity and the linear region of the LVDT according to the electrical conductivity of the core. When the conductivity

becomes greater than 10,000 S/m, the sensitivity decreases. At a conductivity of 6.67E+6 S/m, the sensitivity decreases by 2.3% when the supply frequency is 60 Hz and approximately 6% when the supply frequency is 2,000 Hz. The linear region exhibits slight changes, but no distinct trend is apparent.

Fig. 5(b) presents the sensitivity and the linear region of the LVDT according to the relative permeability of the core. If the permeability decreases, the sensitivity decreases. In particular, this decrease is large when either the conductivity or supply frequency is high. When the permeability is 1,000, if the conductivity is 6.67E+6 S/m and the supply frequency is 2,000 Hz, then the sensitivity decreases by 23% as compared to the peak. When the supply frequency is 60 Hz, the sensitivity decreases by 4.8%. When the sensitivity decreases, the linear region tends to change or expand slightly. Fig. 6(a) presents the changes in the sensitivity and the linear region according to the frequency change of the power supply. When the electrical conductivity is small (8.33 S/m), the sensitivity exhibits almost no change. When the electrical conductivity is 6.67E+6 S/m, if the frequency increases to 1,000 Hz, the sensitivity decreases by up to 3.7%; above 1,000 Hz, the sensitivity does not change further. This implies that the decrease in the sensitivity owing to eddy currents reaches a limit at a high frequency. In the case of high conductivity, if the frequency decreases, then the linear region decreases slightly.

Fig. 6(b) shows that, as the voltage increases, the sensitivity increases proportionally, but the size of the linear region remains constant. When the core's conductivity is large, the sensitivity decreases slightly, and as the voltage increases, the sensitivity further decreases slightly. As the conductivity increases, the linear region increases slightly, but it shows no change when the voltage increases.

Fig. 7 presents the Joule losses inside the core

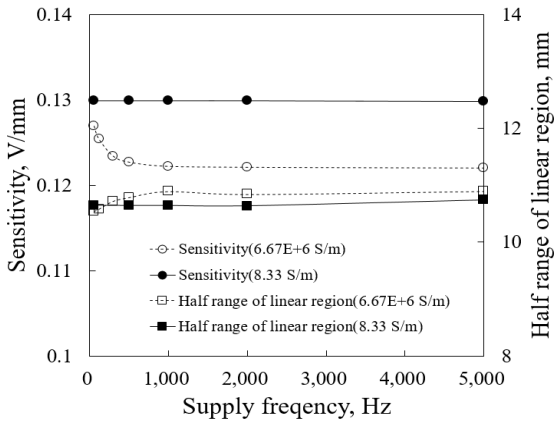

(a) Frequency

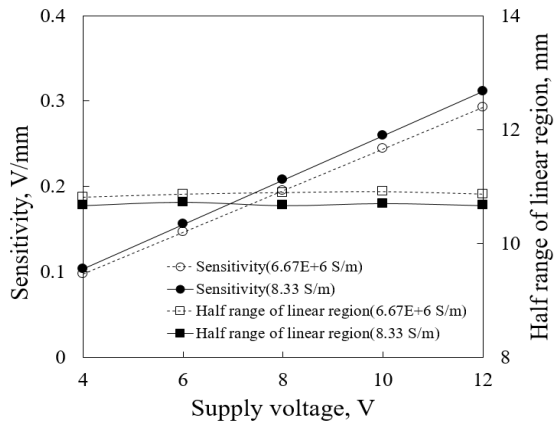

(b) Voltage

Fig. 6 Sensitivity and linear region with changes of process parameter

according to the frequency and permeability changes. The lower the frequency and permeability, the larger the loss is. This indicates that the eddy current flowing in the core is large.

Fig. 8(a) presents the current flowing in the primary coil when the supply voltage is 5 V, the core's electrical conductivity is 6.67E+6 S/m, and the core's relative permeability changes from 1,000 to 20,000. As the permeability increases, the current flowing in the primary coil decreases. When the supply frequency is 2,000 Hz, it decreases from 4.7 mA to 3.3 mA, which comprises a 29.5% reduction.

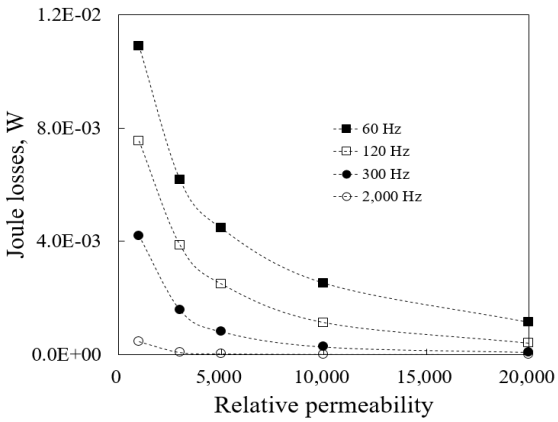

Fig. 7 Joule losses with changes of core permeability and supply frequency

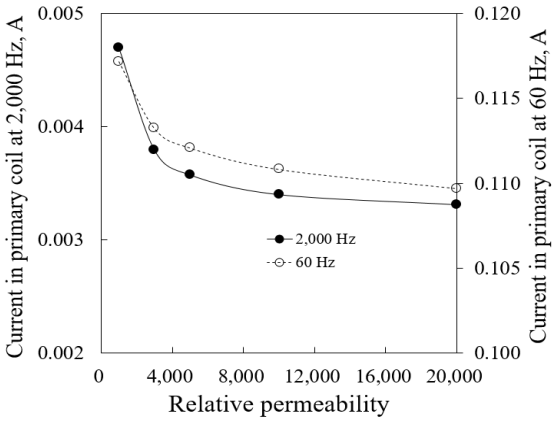

(a) Permeability

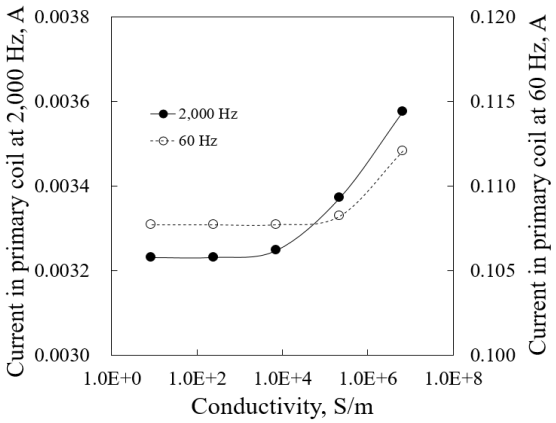

(b) Conductivity

Fig. 8 Current in primary coil with changes of material parameter

When the supply frequency is 60 Hz, it decreases by 6.4% from 117.2 mA to 109.7 mA. When the frequency is large, the current flowing in the primary coil is small, and it decreases further according to the increase in the permeability.

Fig. 8(b) presents the changes in the current of the primary coil according to the electrical conductivity when the supply voltage is 5 V and the core permeability is 5,000. As the electrical conductivity increases, the current flowing in the primary coil also increases. This is determined to be a result of reducing the self-inductance of the primary coil owing to the periodic changes in the eddy current. It decreases by approximately 9.6% from 3.58 mA to 3.23 mA in the case of 2,000 Hz when the conductivity decreases from 6.67E+6 S/m to 8.33 S/m, and it decreases by approximately 3.9% from 112.1 mA to 107.7 mA in the case of 60 Hz. When the frequency is high, the decrease in the current caused by the decrease in the conductivity is greater. This is owing to the high frequency of the eddy current, and it is the reason the decline in the sensitivity is greater.

Fig. 9(a) presents the electromagnetic force according to the core displacement and the change in the voltage for a frequency of 2,000 Hz. It can be observed that, as the voltage increases and the core displacement increases, the electromagnetic force acting in the opposite direction of the displacement increases. The increase in the electromagnetic force is greater than that in the voltage. When the displacement of the core is 0, the electromagnetic force is 0, but as the core displacement increases, the latter increases gradually, and as its behavior is similar to the increase rate of the self-inductance, it is proportional to the inductance increase rate.

Fig. 9(b) presents the change in the electromagnetic

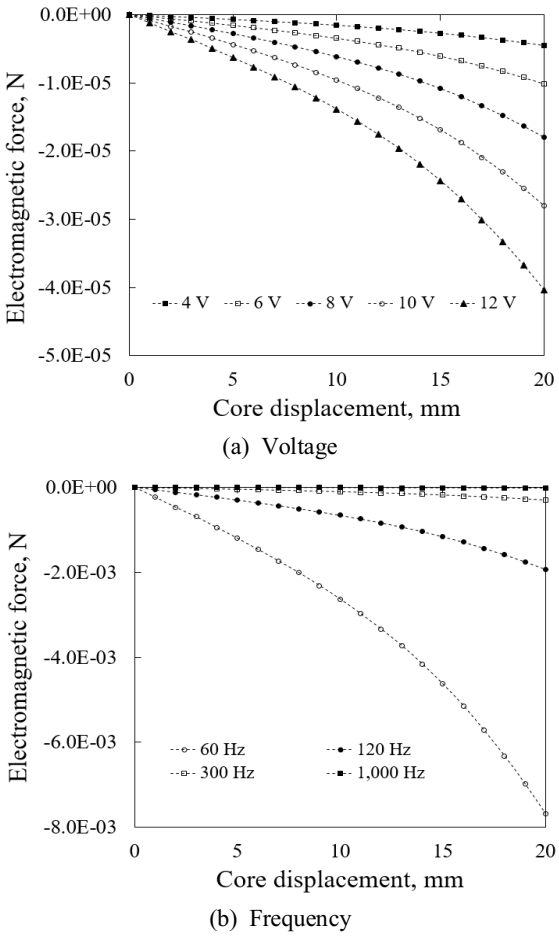

Fig. 9 Electromagnetic force with changes of core displacement for process parameter

force of the core according to the frequency change and core displacement. When the frequency is low, the electromagnetic force is large. This is because, the lower the frequency is, the greater is the current flowing in the primary coil. As the frequency increases, the electromagnetic force decreases sharply. The analysis results obtained on considering the core's permeability change and resistance change are similar to the results presented in Fig. 9. It is determined that the current change of the primary coil occurs owing to the change in the material used; however, the inductance characteristics also change, which offsets the effect on the electromagnetic force.

4. Conclusion

We proposed a finite element analysis model for analyzing the output characteristics of an LVDT according to the process and material parameters. Based on the analysis thus performed, we derived the following conclusions.

1. When the core's electrical conductivity is not taken into consideration, the finite element analysis results are similar to the theoretical analysis results, which verifies the validity of the proposed analysis model.
2. The voltage induced in a secondary coil is determined by the increase in the mutual inductance and the decrease in the self-inductance, both of which are proportional to the square of the core displacement.
3. When the core's electrical conductivity is greater than or equal to 10,000 S/m or the relative permeability is less than or equal to 10,000, the sensitivity decreases. Furthermore, when the electrical conductivity increases further or the permeability decreases further, the decrease in the sensitivity is greater. Here, if the frequency increases, the decrease in the sensitivity is even greater.
4. As the supply voltage increases, the sensitivity increases, and when the electrical conductivity is high, the rate of increase in sensitivity is reduced.
5. When the supply frequency increases, the core's eddy current has a relatively greater impact on the current of the primary coil.
6. The electromagnetic force applied to the core increases parabolically as the voltage increases, the frequency decreases, and core displacement increases.

Acknowledgment

"This work was supported by Gyeongnam National University of Science and Technology Grant in 2020~2021."

REFERENCES

1. Lee, N.-G., Kwac, L.-K. and Kim, H.-G., "A Study on the Universal Outer Diameter Measurement Module using LVDT", Journal of the Korean Society of Manufacturing Process Engineers, Vol. 16, No. 3, pp. 100-106, 2017.
2. Masi, A., Danisi, A., Losito, R., Martino, M. and Spiezia, G., "Study of Magnetic Interference on an LVDT: FEM Modeling and Experimental Measurements", Journal of Sensors, Vol. 2011, pp. 1-9, 2011.
3. Al-Sharif, L., Kilani, M., Taifour, S., Issa, A. J., Al-Qaisi, E., Eleiwi, F. A. and Kamal, O. N., "Linear Variable Differential Transformer Design and Verification Using MATLAB and Finite Element Analysis, Matlab for Engineers", Edited by K. Perutka, IntechWeb.org, pp. 75-94, 2011.
4. Baidwan, K. I. S. and Kumar, C. R. S., "Design of Linear Variable Differential Transformer (LVDT) Based Displacement Sensor with Wider Linear Range Characteristics", The International Journal of Science & Technoledge, Vol. 3, No. 4, pp. 74-79, 2015.
5. Doebelin, E. O., Measurement Systems: Application and Design, McGraw-Hill, New York, 4 ed., 1990.
6. Souza, C. P. and Wanderley, M. B., "Conversion from Geometrical to Electrical Model of LVDT", 16th IMEKO TC4 Symposium, Exploring New Frontiers of Instrumentation and Methods for Electrical and Electronic Measurements, pp. 22-24, Florence, Italy, 2008.
7. Techical Report, Development of Domestic LVDTs for Precision Measurement, Korea Standards Research Institute, 1989.
8. Techical Report, Basic Design of Radiation-Resistant LVDTs, Korea Atomic Energy Research Institute, 2008.
9. Yanez-Valdez, R., Alva-Gallegos, R., Caballero-Ruiz, A. and Ruiz-Huerta, L., "Selection of Soft Magnetic Core Materials Used on an LVDT Prototype", Journal of Applied Research and Technology, Vol. 10, No. 2, pp. 195-205, 2012.
10. Han, E.-G., Choi, M.-Y., Chang, K.-Y. and Noh, B.-W., Precision Measurement Technology, Dongil Press, Ch. 3, pp. 108-117, 1998.
11. FluxTM 2020, 3D Applications User's Guide, Altair Engineering Inc., Troy, Michigan, USA, 2020.